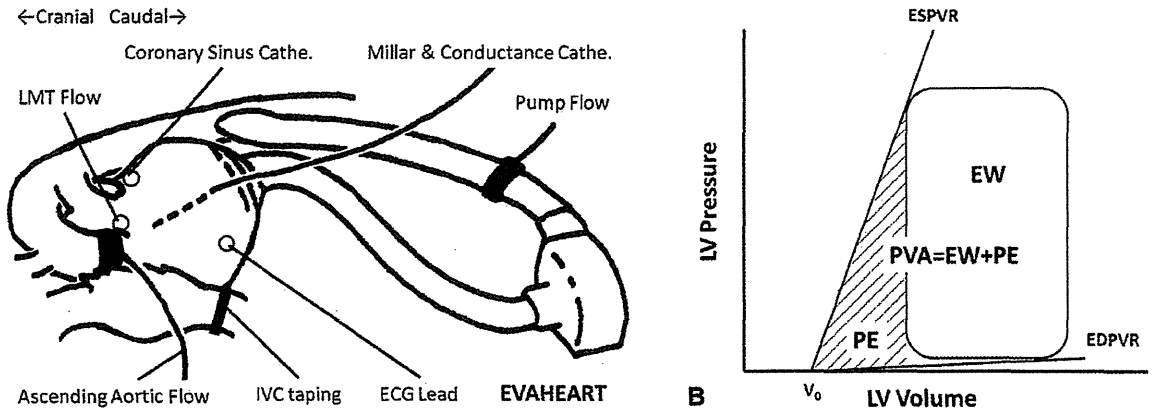

FIGURE 1. A, Experimental settings. B, PV loop. PVA is the sum of external work and potential energy. *LMT*, Left main trunk (of the coronary artery); *IVC*, inferior vena cava; *ECG*, electrocardiogram; *ESPVR*, end-systolic pressure volume relationship; *LV*, left ventricular; *EW*, external work; *PE*, potential energy; *PVA*, pressure volume area; *EDPVR*, end-diastolic pressure volume relationship; V_0, X axis intercept of the end-systolic PV relationship slope.

Myocardial Oxygen Consumption Assessment

We calculated MVO2 for evaluation of LV workload.[16,18-20] A 10F retrograde cardioplegic catheter (Gandry RCSP catheter, 94110, Medtronic Japan Co, Ltd, Tokyo, Japan) was inserted into the coronary sinus through the hemiazygos vein. A balloon was inflated, and coronary vein blood was drawn via a small hole created manually just before a balloon to avoid collecting mixed central venous blood.[18] We calculated MVO2 by the following formula: MVO2 (O2 mL/min) = {(ScaO2 − ScvO2) · 1.34 · aHb + (PcaO2 − PcvO2) · 0.003} · 0.01 · coronary flow, where ScaO2 (ScvO2) is the oxygen saturation of coronary artery (vein) blood, PcaO2 (PcvO2), mm Hg is the partial pressure of coronary artery (vein) blood, and aHb, g/dL is the hemoglobin concentration of coronary artery blood.

We calculated normalized MVO2 per beat per 100 g of LV tissue. Data are presented as percentages of those in the circuit clamp, taken as 100%.

Pressure Volume Area Assessment

The Sigma5 DF system (CD Leycom, Zoetermeer, The Netherlands) was used for PV loop analysis. The end-systolic PV relationship slope was obtained by gradually occluding the inferior vena cava. PVA, recognized as a measure of total mechanical energy,[19,20] was approximated using a previously established method.[20,21] Briefly, external work is a computed area in the loop and potential energy is a crescent-shaped area between the end-systolic PV relationship slope and isovolumic relaxation (Figure 1, *B*). PVA, the sum of external work and potential energy, is shown as the normalized value per 100 g of LV tissue.[20] We also evaluated end-systolic pressure, end-systolic volume (ESV), end-diastolic pressure (EDP), and end-diastolic volume (EDV). We drew blood and performed calibration with a conductivity meter. However, the absolute LV volume value does not reflect actual LV volume. Therefore, we evaluated these data by comparative assessment with LV volume under circuit-clamp conditions as the baseline (100%). LV pressure data are also presented as percent values.

Statistical Analysis

All numeric data are shown as average ± standard deviation. Comparisons between groups were performed by repeated-measures analysis of variance followed by Tukey's multiple comparison test. All analyses were conducted using a 2-sided method. The efficacy outcome measure was the retrograde PF amount. We specified a minimum detectable difference in retrograde PF of 0.75 L/min (the difference between a mean of 1.40 L/min for continuous mode and 0.65 L/min for off-test mode). Therefore, a sample size of 8 was selected to ensure 80% power for detecting the specified minimum difference at a 2-sided significance level of .05. We used PASW Statistics18 (IBM SPSS Inc, Chicago, Ill) for all statistical analyses.

RESULTS

Figure 2 shows sample waveforms of pressure and flow data. In continuous mode, diastolic reverse PF was observed and diastolic AoP shifted upward compared with the circuit clamp (Figure 2). While in off-test mode, diastolic RPM was increased by synchronization and the reversal of PF almost completely disappeared. Diastolic AoP was maintained in off-test mode.

Table 1 shows numeric flow and pressure data. There was no significant change in heart rate, mean CVP, mean AoP, or mean LV pressure. In continuous mode, RPM was approximately 990 and PF was 0.19 L/min (Table 1). In off-test mode, systolic RPM was 690 and diastolic RPM was 1320. PF increased to 0.66 from 0.19 L/min in continuous mode, but the difference was not significant. In off-test mode, AoF was significantly decreased and the bypass rate was significantly increased compared with continuous mode (Table 1).

PV loops are shown in Figure 3. In continuous mode, both end-systolic and diastolic points were shifted rightward compared with the circuit-clamp. End-diastolic points also shifted upward. While in off-test mode, the loop was similar to that under circuit-clamp conditions. Ventricular pressures and volumes are shown in Figure 4. In continuous mode, %EDP was increased ($P = .001$). %EDP decreased in off-test mode, but the difference was not significant ($P = .08$). Both %EDV and %ESV increased in continuous mode, but these differences also did not reach statistical significance.

%PVA and %MVO2 in each mode are shown in Figure 5, *A*. %PVA increased in continuous mode, but the difference was not significant. In off-test mode, %PVA

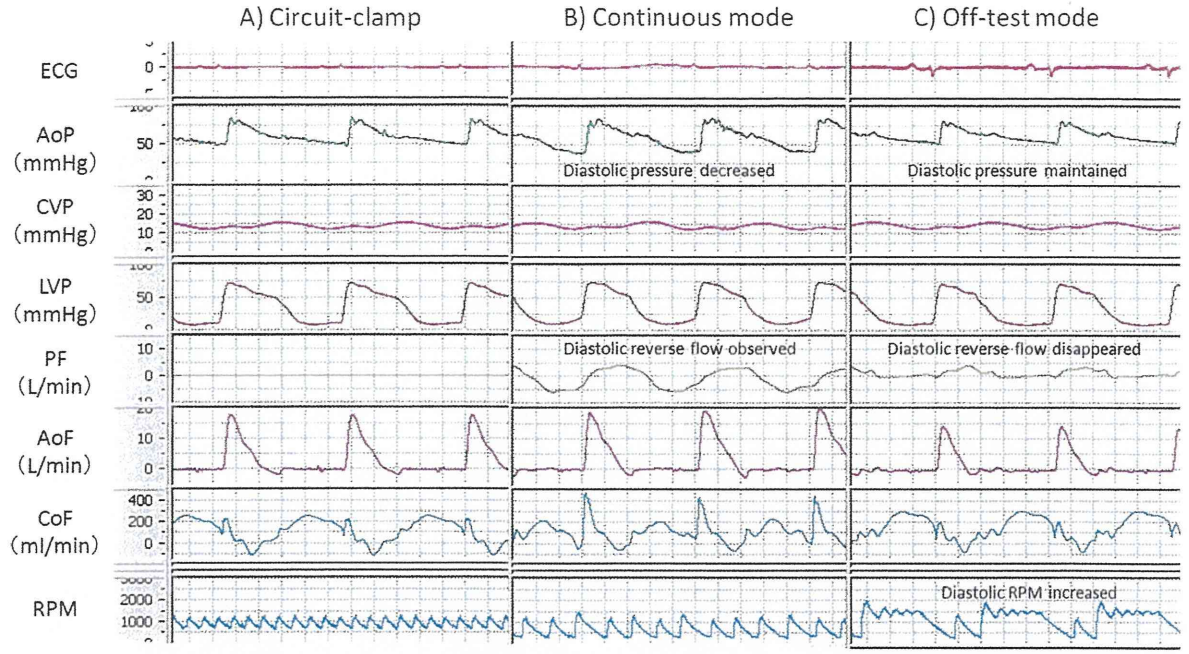

FIGURE 2. Pressure and flow waveforms. In continuous mode, diastolic reverse PF was observed. However in off-test mode, diastolic RPM increased and the reversal of PF disappeared completely. *ECG*, Electrocardiogram; *AoP*, aortic pressure; *CVP*, central venous pressure; *LVP*, left ventricular pressure; *PF*, pump flow; *AoF*, ascending aortic flow; *CoF*, coronary flow; *RPM*, revolution per minute.

and %MVO2 were both similar to corresponding values under circuit-clamp conditions. The amount of retrograde PF in each mode is shown in Figure 5, *B*. In continuous mode, the amount was 1.38 ± 0.62 L/min, and significantly decreased to 0.66 ± 0.57 L/min ($P = .005$) in off-test mode.

DISCUSSION

Our ultimate goal is to establish a safe and appropriate weaning protocol for rotary LVAD removal. Our novel drive mode that can change pump RPM via synchronization successfully reduced the amount of retrograde PF in diastole during pump weaning while keeping LV workload similar to that under circuit-clamp conditions. These data raise the possibility of mimicking circuit-clamp conditions while evaluating native heart function before LVAD removal, even in rotary LVADs implanted intracorporeally. These findings are both unique and clinically relevant.

TABLE 1. Flow and pressure data

Mode	Circuit clamp	Continuous mode	Off-test mode
Heart rate (rpm)	78.0 ± 13.8	77.9 ± 13.5	75.6 ± 13.9
Mean CVP (mm Hg)	11.8 ± 5.3	11.7 ± 4.9	12.3 ± 4.6
Mean AoP (mm Hg)	62.4 ± 11.2	56.3 ± 8.8	57.1 ± 12.4
Mean LVP (mm Hg)	38.9 ± 11.7	38.9 ± 11.4	37.5 ± 10.7
Systolic RPM	0.0 ± 0.0	990 ± 210*	690 ± 60*,†
Diastolic RPM	0.0 ± 0.0	990 ± 210*	1320 ± 290*,†
Mean RPM	0.0 ± 0.0	960 ± 190*	1060 ± 210*
PF (L/min)	0.00 ± 0.00	0.19 ± 0.37	0.66 ± 0.85
AoF (L/min)	3.94 ± 1.93	3.68 ± 1.89	2.75 ± 1.32*,†
Bypass rate (%)	0.0 ± 0.0	5.7 ± 10.6	19.5 ± 14.5*,†

LVP, Left ventricular pressure. *Significant change from circuit-clamp condition. †Significant change from continuous mode.

In addition to the weaning protocol, other factors, such as patient selection and effective adjunctive therapies, are clearly of great significance. Dandel and colleagues[4] reported pre-explantation factors, including duration of LVAD support, heart failure duration before LVAD implantation, and echocardiographic findings, to predict cardiac stability after LVAD removal. Birks and colleagues[3,9] have suggested the importance of medical therapy, including the beta-2 agonist clenbuterol in combination with mechanical support.[3,9] Other medical therapies,[22] resynchronization therapy,[23] or rehabilitation[23] during VAD support augment the rate of successful removal. In the near future, even molecular changes occurring during reverse remodeling might be of value in assessing device withdrawal.[24] Nevertheless, creating or mimicking no-support circumstances before removal would likely still be necessary.

Figure 2 shows sample pressure and waveforms. In continuous mode, retrograde PF persisted and diastolic AoP was shifted downward, possibly because of this retrograde PF. In off-test mode, the amount of retrograde PF decreased as diastolic RPM increased, and diastolic AoP was similar to that under circuit-clamp condition. Comparing PF wave forms between continuous and off-test modes showed

ET/BS

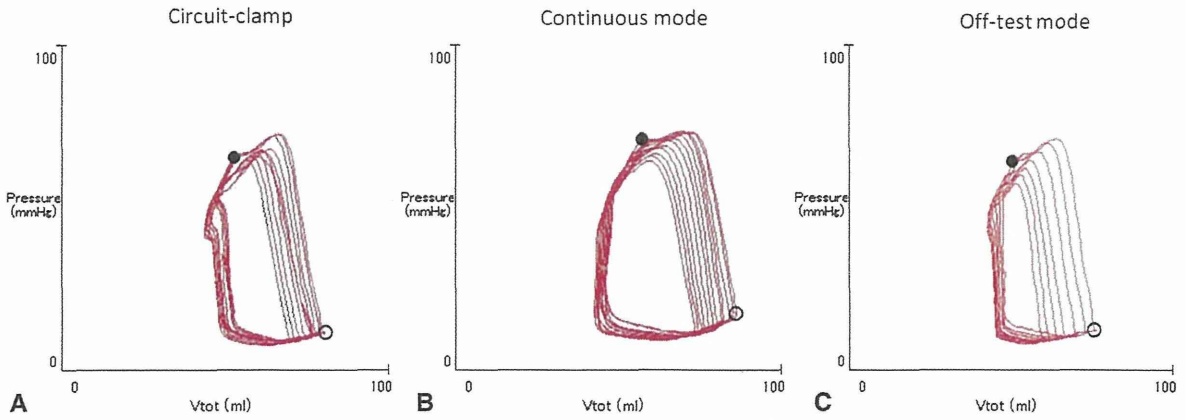

FIGURE 3. PV loops. End-systolic point (*black dot*) and end-diastolic point (*white circle*). In continuous mode, end-systolic and end-diastolic points are shifted rightward compared with circuit-clamp conditions. End-diastolic points are shifted upward. In off-test mode, the loop is similar to that in circuit-clamp condition.

almost zero PF, whereas continuous mode showed "zero net flow," meaning certain amounts of both forward and backward flow persisted. While in off-test mode, an almost flat PF waveform was obtained, and this mode showed "zero-total-flow in the circuit," as if the circuit was clamped. This was the PF waveform we were endeavoring to achieve in the current study (Figure 2).

The coronary flow waveform in off-test mode was similar to that under circuit-clamp conditions, whereas that in continuous mode was entirely different from those in the other 2 states, in that diastolic coronary flow was decreased (Figure 2). We speculate that in continuous mode, LVED pressure was increased because of retrograde PF (Figure 4), and diastolic coronary flow could

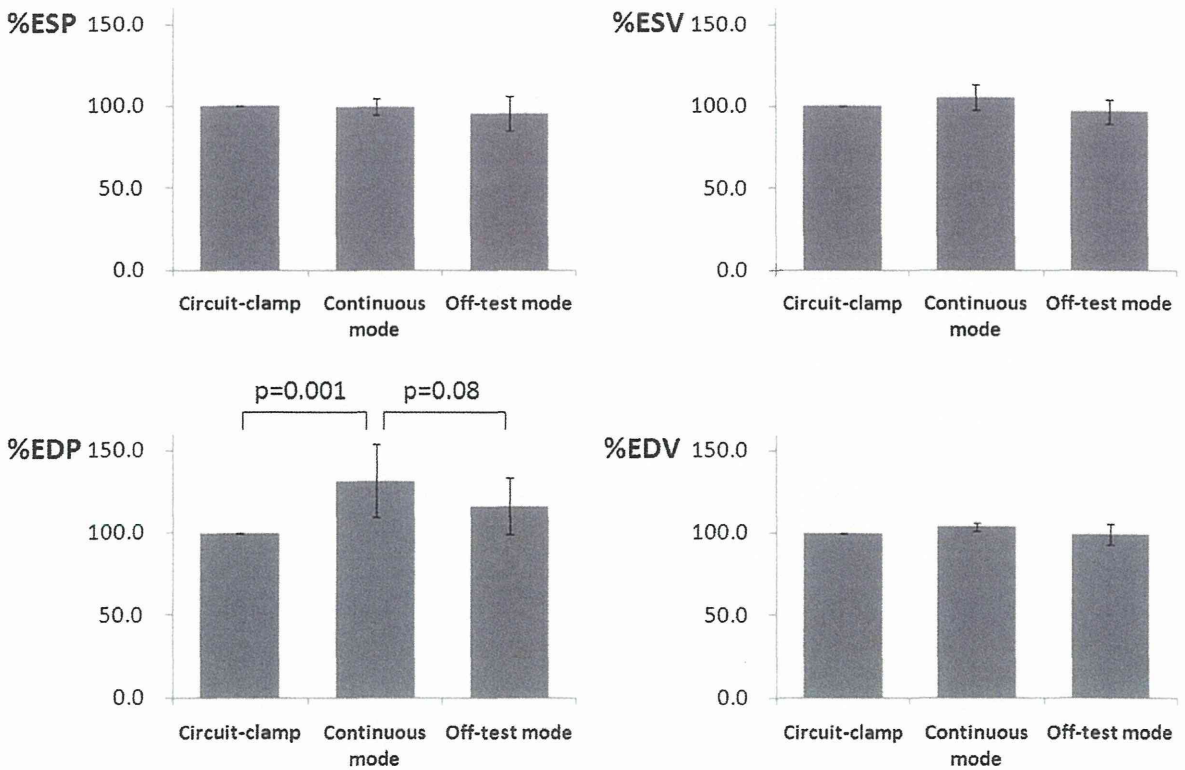

FIGURE 4. LV pressure and volume data. These parameters are shown as percentages of values under circuit-clamp conditions as baseline (100%). %EDP was significantly increased in continuous mode compared with circuit-clamp conditions. *ESP*, End-systolic pressure; *ESV*, end-systolic volume; *EDP*, end-diastolic pressure; *EDV*, end-diastolic volume.

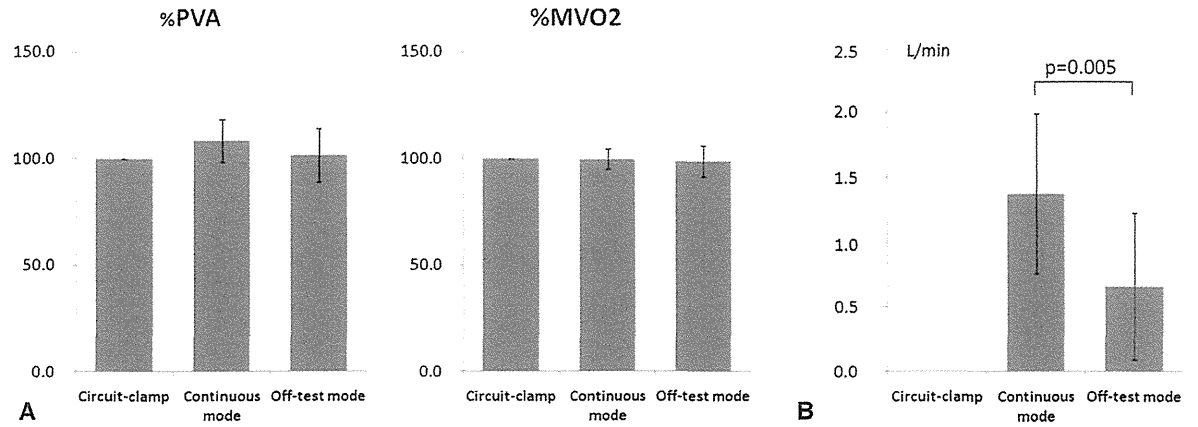

FIGURE 5. A, PVA and MVO2. There were no significant changes in PVA or MVO2 in any of the 3 modes. B, Retrograde PF. In continuous mode, the amount of reverse PF was 1.38 L/min. However, this was significantly decreased to 0.66 L/min in off-test mode. *PVA*, Pressure volume area; *MVO2*, myocardial oxygen consumption.

have been decreased by increased intramural pressure.[19,25]

Table 1 shows flow and pressure numeric data. There were no changes in heart rate, CVP, AoP, or LV pressure. In off-test mode, PF was increased compared with continuous mode. This change, attributed to reduced retrograde PF, was not significant. In off-test mode, AoF was significantly decreased (Table 1). This AoF decrease may have also been due to reduced retrograde PF. The present study used a normal heart model, such that in continuous mode the native heart could compensate for backward flow by increasing AoF. This compensation could represent an excessive load on the native heart during pump weaning. While in off-test mode, there was almost no reverse flow, making compensation by the native heart unnecessary. In the systolic phase, it would be natural for a small amount of forward flow to occur in off-test mode (Figure 2), because the pump circuit is open. We believe this systolic forward flow was ejected mostly by the native heart because systolic RPM in off-test mode was set at 700, the minimum RPM in the current system (Table 1).

Figure 3 shows sample PV loops, and Figure 5, *A*, shows changes in %PVA and %MVO2. We were successful in obtaining similar PV loops in off-test mode and circuit-clamp states, meaning that the native heart workload was almost the same in these 2 settings (Figure 5, *A*). In continuous mode, the PV loop was larger than under the other 2 conditions, but this change was not significant. We speculate that the lack of significant change in LV workload is attributable to good ventricular function. The results would have been different had we conducted the same investigation in a heart failure model. Figure 4 shows LV pressure and volume. In continuous mode, EDP was significantly increased compared with circuit-clamp conditions ($P = .001$), and off-test mode blunted this elevation in EDP ($P = .08$). EDV and ESV were unchanged, possibly because of low compliance of the native heart and the rate of LV volume change. In continuous mode, EDP occasionally doubled, for example, from 10 to 20 mm Hg, but there was no increase in EDV or ESV even with such a large change. Figure 5, *B*, shows changes in retrograde PF, indicating off-test mode to successfully reduce retrograde PF. The retrograde PF difference between the 2 modes was modest, but this difference might be larger in heart failure models, possibly affecting native heart recovery.

There have been clinical reports describing pump-off trials after myocardial recovery.[3,4,8,11] In patients with pulsatile pumps, Mano and colleagues[8] conducted dobutamine stress testing under minimal support with pulsatile LVADs, driven at 60 beats/min. Dandel and colleagues[4] performed 10-minute echocardiography under support at 1 beat/min, which necessitated systemic heparinization. With most pulsatile LVADs, there is little concern about retrograde PF because of the mechanical valves in circuits, and with commonly used pulsatile pumps, such as the Heartmate XVE (Thoratec Corp, Pleasanton, Calif), pump-off trials can be attempted using intermittent hand pumping with systemic anticoagulation. However, these trials should be done relatively quickly to avoid intracircuit clotting. With rotary LVADs, attempts have been made to adjust pump RPM to achieve "zero net flow" condition, tolerating both forward and backward flows in the circuit.[4] However, this approach to pump weaning raises concerns, because retrograde PF in diastole might overload the native heart and even be misleading for cardiac evaluation.[10] As shown in the current study, continuous mode with low RPM actually created a certain amount of retrograde PF (Figure 2), and our off-test mode blunted this retrograde PF.

Even in the current era, weaning tests should be done on admission under careful monitoring with a pulmonary artery catheter and echocardiography, relatively quickly because of the aforementioned retrograde PF during

weaning. However, our off-test mode decreased this reverse flow in a normal heart model. Before the clinical application of this system, we must clarify its utility in heart failure models. In the near future, it should be possible to more safely maintain this mode for a relatively long time, even a few months. Our ultimate goal is establish a safe and appropriate weaning protocol for LVAD withdrawal that can be carried out in the outpatient setting. The aims of an off-test trial in the outpatient clinic would be (1) to allow more time to safely decide on withdrawal, with careful patient selection; (2) to take into account patients' activities of daily living and symptoms in their own daily lives before pump removal; and (3) to develop a reversible mode allowing a return to full support conditions in the event of worsening patient status.

Study Limitations

The present study has several limitations. First, we need to establish the method of actual adjustment of diastolic RPM in the clinical setting. With the current system, PF monitoring during pump support is difficult. In practice, we were able to measure the amount of retrograde PF by echocardiography in the outpatient clinic, allowing diastolic RPM to be adjusted. Second, our mode might result in stagnant flow within the circuit. Therefore, we must provide adequate anticoagulation with Coumadin (Bristol-Myers Squibb, Princeton, NJ) while using the off-test mode. Otherwise, intracircuit stagnant flow might be washed out by intermittently increasing RPM. A study for evaluating chronic thrombus formation is currently ongoing. Third, the study was conducted using a normal heart model and a relatively small sample number of animals. We will next focus on a heart failure model, in which the native heart cannot compensate for retrograde PF in continuous mode, such that PVA and MVO2 will increase more than in the present study. Further investigations will examine chronic heart failure models and include larger sample sizes, providing more information on clotting or device durability.

CONCLUSIONS

Our newly developed off-test mode for centrifugal LVADs can decrease retrograde PF during pump weaning while keeping LV workload similar to that under circuit-clamp conditions. This mode is of potential value in establishing a safe and appropriate LVAD weaning protocol after myocardial recovery. Further investigation in chronic heart failure models is currently ongoing.

References

1. Slaughter MS, Rogers JG, Milano CA, Russell SD, Conte JV, Feldman D, et al. Advanced heart failure treated with continuous-flow left ventricular assist device. *N Engl J Med.* 2009;361:2241-51.
2. Lahpor J, Khaghani A, Hetzer R, Pavie A, Friedrich I, Sander K, et al. European results with a continuous-flow ventricular assist device for advanced heart-failure patients. *Eur J Cardiothorac Surg.* 2010;37:357-61.
3. Birks EJ, Tansley PD, Hardy J, George RS, Bowles CT, Burke M, et al. Left ventricular assist device and drug therapy for the reversal of heart failure. *N Engl J Med.* 2006;355:1873-84.
4. Dandel M, Weng Y, Siniawski H, Potapov E, Drews T, Lehmkuhl HB, et al. Prediction of cardiac stability after weaning from left ventricular assist devices in patients with idiopathic dilated cardiomyopathy. *Circulation.* 2008;118: S94-105.
5. Matsumiya G, Monta O, Fukushima N, Sawa Y, Funatsu T, Toda K, et al. Who would be a candidate for bridge to recovery during prolonged mechanical left ventricular support in idiopathic dilated cardiomyopathy? *J Thorac Cardiovasc Surg.* 2005;130:699-704.
6. Mokashi SA, Guan J, Wang D, Tchantchaleishvili V, Brigham M, Lipsitz S, et al. Preventing cardiac remodeling: the combination of cell-based therapy and cardiac support therapy preserves left ventricular function in rodent model of myocardial ischemia. *J Thorac Cardiovasc Surg.* 2010;140:1374-80.
7. Korf-Klingebiel M, Kempf T, Schluter KD, Willenbockel C, Brod T, Heineke J, et al. Conditional transgenic expression of fibroblast growth factor 9 in the adult mouse heart reduces heart failure mortality after myocardial infarction. *Circulation.* 2011;123:504-14.
8. Mano A, Nakatani T, Oda N, Kato T, Niwaya K, Tagusari O, et al. Which factors predict the recovery of natural heart function after insertion of a left ventricular assist system? *J Heart Lung Transplant.* 2008;27:869-74.
9. Birks EJ, George RS, Hedger M, Bahrami T, Wilton P, Bowles CT, et al. Reversal of severe heart failure with a continuous-flow left ventricular assist device and pharmacological therapy: a prospective study. *Circulation.* 2011;123:381-90.
10. Schima H, Vollkron M, Boehm H, Rothy W, Haisjackl M, Wieselthaler G, et al. Weaning of rotary blood pump recipients after myocardial recovery: a computer study of changes in cardiac energetics. *J Thorac Cardiovasc Surg.* 2004;127:1743-50.
11. Myers TJ, Frazier OH, Mesina HS, Radovancevic B, Gregoric ID. Hemodynamics and patient safety during pump-off studies of an axial-flow left ventricular assist device. *J Heart Lung Transplant.* 2006;25:379-83.
12. Ando M, Nishimura T, Takewa Y, Ogawa D, Yamazaki K, Kashiwa K, et al. What is the ideal off-test trial for continuous-flow ventricular-assist-device explantation? Intracircuit back-flow analysis in a mock circulation model. *J Artif Organs.* 2011;14:70-3. Epub 2011 Jan 18.
13. Ando M, Nishimura T, Takewa Y, Ogawa D, Yamazaki K, Kashiwa K, et al. A novel counterpulse drive mode of continuous-flow left ventricular assist devices can minimize intracircuit backward flow during pump weaning. *J Artif Organs.* 2011;14:74-9. Epub 2011 Jan 18.
14. Yamazaki K, Saito S, Kihara S, Tagusari O, Kurosawa H. Completely pulsatile high flow circulatory support with a constant-speed centrifugal blood pump: mechanisms and early clinical observations. *Gen Thorac Cardiovasc Surg.* 2007;55:158-62.
15. Kitamura M, Hanzawa K, Aoki K, Saitoh M, Hayashi J. Direct cardiac potential trigger for chronic control of a ventricular assist device. *ASAIO J.* 2001;47:302-4.
16. Ando M, Nishimura T, Takewa Y, Yamazaki K, Kyo S, Ono M, et al. Electrocardiogram-synchronized rotational speed change mode in rotary pumps could improve pulsatility. *Artif Organs.* 2011;35:941-7.
17. Ando M, Takewa Y, Nishimura T, Yamazaki K, Kyo S, Ono M, et al. A novel counterpulsation mode of rotary left ventricular assist devices can enhance myocardial perfusion. *J Artif Organs.* 2011;14:185-91.
18. Tuzun E, Eya K, Chee HK, Conger JL, Bruno NK, Frazier OH, et al. Myocardial hemodynamics, physiology, and perfusion with an axial flow left ventricular assist device in the calf. *ASAIO J.* 2004;50:47-53.
19. Tune JD, Gorman MW, Feigl EO. Matching coronary blood flow to myocardial oxygen consumption. *J Appl Physiol.* 2004;97:404-15.
20. Suga H, Hayashi T, Shirahata M. Ventricular systolic pressure-volume area as predictor of cardiac oxygen consumption. *Am J Physiol.* 1981;240:H39-44.
21. Ueno A, Tomizawa Y. Cardiac rehabilitation and artificial heart devices. *J Artif Organs.* 2009;12:90-7.
22. Nishimura T, Kyo S. High-dose carvedilol therapy for mechanical circulatory assisted patients. *J Artif Organs.* 2010;13:88-91.
23. Nishimura T, Kyo S. Triple-site pacing: a new supported therapy approach for bridge to recovery with a left ventricular assist system in a patient with idiopathic dilated cardiomyopathy. *J Artif Organs.* 2010;13:54-7.
24. Birks EJ, George RS. Molecular changes occurring during reverse remodelling following left ventricular assist device support. *J Cardiovasc Transl Res.* 2010; 3:635-42.
25. Elhabyan AK, Reyes BJ, Hallak O, Broce M, Rosencrance JG, Lucas BD, et al. Subendocardial ischemia without coronary artery disease: is elevated left ventricular end diastolic pressure the culprit? *Curr Med Res Opin.* 2004;20:773-7.

J Artif Organs
DOI 10.1007/s10047-012-0679-8

ORIGINAL ARTICLE

In vivo evaluation of an in-body, tissue-engineered, completely autologous valved conduit (biovalve type VI) as an aortic valve in a goat model

Yoshiaki Takewa · Masashi Yamanami · Yuichiro Kishimoto · Mamoru Arakawa · Keiichi Kanda · Yuichi Matsui · Tomonori Oie · Hatsue Ishibashi-Ueda · Tsutomu Tajikawa · Kenkichi Ohba · Hitoshi Yaku · Yoshiyuki Taenaka · Eisuke Tatsumi · Yasuhide Nakayama

Received: 14 February 2012 / Accepted: 25 November 2012

Abstract Using simple, safe, and economical in-body tissue engineering, autologous valved conduits (biovalves) with the sinus of Valsalva and without any artificial support materials were developed in animal recipients' bodies. In this study, the feasibility of the biovalve as an aortic valve was evaluated in a goat model. Biovalves were prepared by 2-month embedding of the molds, assembled using two types of specially designed plastic rods, in the dorsal subcutaneous spaces of goats. One rod had three projections, resembling the protrusions of the sinus of Valsalva. Completely autologous connective tissue biovalves (type VI) with three leaflets in the inner side of the conduit with the sinus of Valsalva were obtained after removing the molds from both terminals of the harvested implants with complete encapsulation. The biovalve leaflets had appropriate strength and elastic characteristics similar to those of native aortic valves; thus, a robust conduit was formed. Tight valvular coaptation and a sufficient open orifice area were observed in vitro. Biovalves ($n = 3$) were implanted in the specially designed apico-aortic bypass for 2 months as a pilot study. Postoperative echocardiography showed smooth movement of the leaflets with little regurgitation under systemic circulation (2.6 ± 1.1 l/min). α-SMA–positive cells appeared significantly with rich angiogenesis in the conduit and expanded toward the leaflet tip. At the sinus portions, marked elastic fibers were formed. The luminal surface was covered with thin pseudointima without thrombus formation. Completely autologous biovalves with robust and elastic characteristics satisfied the higher requirements of the systemic circulation in goats for 2 months with the potential for valvular tissue regeneration.

Keywords In vivo tissue engineering · Heart valve · Autologous tissue · Aortic valve · Systemic circulation

Y. Takewa (✉) · Y. Kishimoto · M. Arakawa · Y. Taenaka · E. Tatsumi
Department of Artificial Organs, National Cerebral and Cardiovascular Center Research Institute, 5-7-1 Fujishiro-dai, Suita, Osaka 565-8565, Japan
e-mail: takewa@ri.ncvc.go.jp

E. Tatsumi
e-mail: tatsumi@ri.ncvc.go.jp

M. Yamanami · Y. Matsui · T. Oie · Y. Nakayama (✉)
Division of Medical Engineering and Materials, National Cerebral and Cardiovascular Center Research Institute, 5-7-1 Fujishiro-dai, Suita, Osaka 565-8565, Japan
e-mail: nakayama@ri.ncvc.go.jp

M. Yamanami · K. Kanda · H. Yaku
Department of Cardiovascular Surgery, Kyoto Prefectural University of Medicine, Kyoto, Japan

Y. Matsui · T. Tajikawa · K. Ohba
Department of Mechanical and Systems Engineering, Kansai University, Osaka, Japan

T. Oie
Shinkan Kogyo Co., Osaka, Japan

H. Ishibashi-Ueda
Department of Pathology, National Cerebral and Cardiovascular Center Hospital, Osaka, Japan

Introduction

Prosthetic valve replacement is a common treatment for severe valvular heart disease. There is a tendency to select bioprosthetic valves over mechanical valves. A major advantage of using bioprosthetic devices is that administration of anticoagulants such as warfarin is not required; however, disadvantages include time-related structural deterioration and pathogenicity (e.g., mad cow disease) [1].

Published online: 20 December 2012

Bioprosthetic devices are usually heterologous (made of bovine pericardia or porcine valves) and require chemical treatment to reduce immunogenicity, which could accelerate their degeneration, including calcification and/or time-related functional failure. Advances in biotechnology and tissue engineering may provide promising solutions to overcome the limitations of current heart valve substitutes [2–4]. Recently, autologous bioprostheses with enhanced maturation characteristics such as anticoagulation, self-repair, tissue regeneration, and growth adaptability have been developed using in vitro tissue engineering technology. Some investigators have successfully implanted in vitro tissue-engineered heart valves (TEHV) in animals and humans by using either decellularized natural tissues [3] or biodegradable synthetic polymers as scaffolds [2]. More recently, allogeneic TEHVs were successfully used for aortic root replacement in lambs [5].

To develop autologous prosthetic tissues that can endure high pressures, we have been focusing on the use of in-body tissue architecture technology [6–9], which is a novel concept in regenerative medicine based on the phenomenon of tissue encapsulation of foreign materials in living bodies. This technology involves the use of living bodies as a reactor and is simple, safe, and cost-effective. Since 2007, we have used in-body tissue architecture technology to develop a series of autologous trileaflet heart valves, called biovalves [10–12]. Last year, a type V biovalve, made of tissues completely autologous with the sinus of Valsalva, was shown to successfully function as an allogeneic conduit valve in the pulmonary valve position for up to 3 months in beagle models [13]. Recently, we have developed a type VI biovalve that did not need pretreatment before implantation by altering the design concept of the mold used to prepare the biovalves so that the trileaflet was obtained in the open form (unpublished data). In this study, the possibility of the type VI biovalve as an aortic valve was evaluated by implantation at the apico-aortic bypass in a goat model as a pilot study.

Methods

Preparation of biovalves

All animals received care according to the Principles of Laboratory Animal Care (formulated by the National Institutes of Health, publication no. 56-23, received 1985), and the research protocol (no. 22-2-4) was approved by the ethics committee of the National Cerebral and Cardiovascular Center.

Three goats (aged 1–2 years; body weight 40–50 kg) were used in this study. A specially designed concave acrylate rod (diameter 16 mm; length 35 mm; Fig. 1a) and convex silicone rod (diameter 16 mm; length 37 mm; Fig. 1a) were assembled with a small 0.5-mm aperture to prepare a cylindrical mold for the biovalve organization (Fig. 1b). The mold was designed to separate the leaflets from each other in the open form. The concave-shaped rod had three removable projections that resembled the three protrusions of the sinus of Valsalva. We placed eight molds into the dorsal subcutaneous pouches of each of the three goats (a total of 24 biovalves) under anesthesia that was induced with 10 mg/kg of ketamine and maintained with 1–3 % isoflurane. After 2 months had elapsed (Fig. 1c), we harvested the implants, which were completely encapsulated with robust connective tissue (Fig. 1d). After treatment with 0.6 % glutaraldehyde for 10 min, the rods were removed from both ends of the developed tubular tissue; furthermore, the type VI biovalves with three protrusions resembling the sinus of Valsalva were well formed. Three membranous leaflets from the inside of the conduit were obtained separately (Fig. 1d). Three out of 24 biovalves were used for transplantation, and the rest were used for evaluation of valve motion characteristics ($n = 6$), mechanical properties ($n = 9$), and histological examination ($n = 6$).

In vitro valve motion

The motion of the biovalve leaflets was recorded using a video camera at a frequency of 20 frames per second and was analyzed in conjunction with the circuit flow pattern by using a modified Windkessel pulsatile flow circuit model used in our previous study [14] (working fluid 0.9 % saline; pulsatile rate 62 bpm; flow rate 627 ml/min). The Reynolds and Womersley numbers were 956–1195 and 10.3–11.7, respectively, and were calculated under heart rates ranging from 70 to 90. We used the cardiac output averaged bypass flow, which is generally 80 ml/min per body weight (kg). The upper pressure was set at 120–150 mmHg and lower pressure at 50–80 mmHg as the systolic and diastolic aortic pressure.

Mechanical properties

Biovalves and native aortic valves ($n = 3$) were used as samples. The native aortic valve was simultaneously obtained from each goat when the 2-month implanted biovalve was harvested. The mechanical properties of the leaflets and conduits were measured using a tensile tester. The samples were cut in a circumferential direction and opened. Tissue specimens, 7 × 7 mm, were tested in humid conditions under a tissue extension rate of 3 mm/min. The ultimate tensile strength and elongation at breaking, indicative of tissue strength and tissue extensibility, respectively, were obtained from the stress-strain curves. The modulus, indicative of tissue stiffness, was calculated as the slope of the linear part of the stress-strain curves.

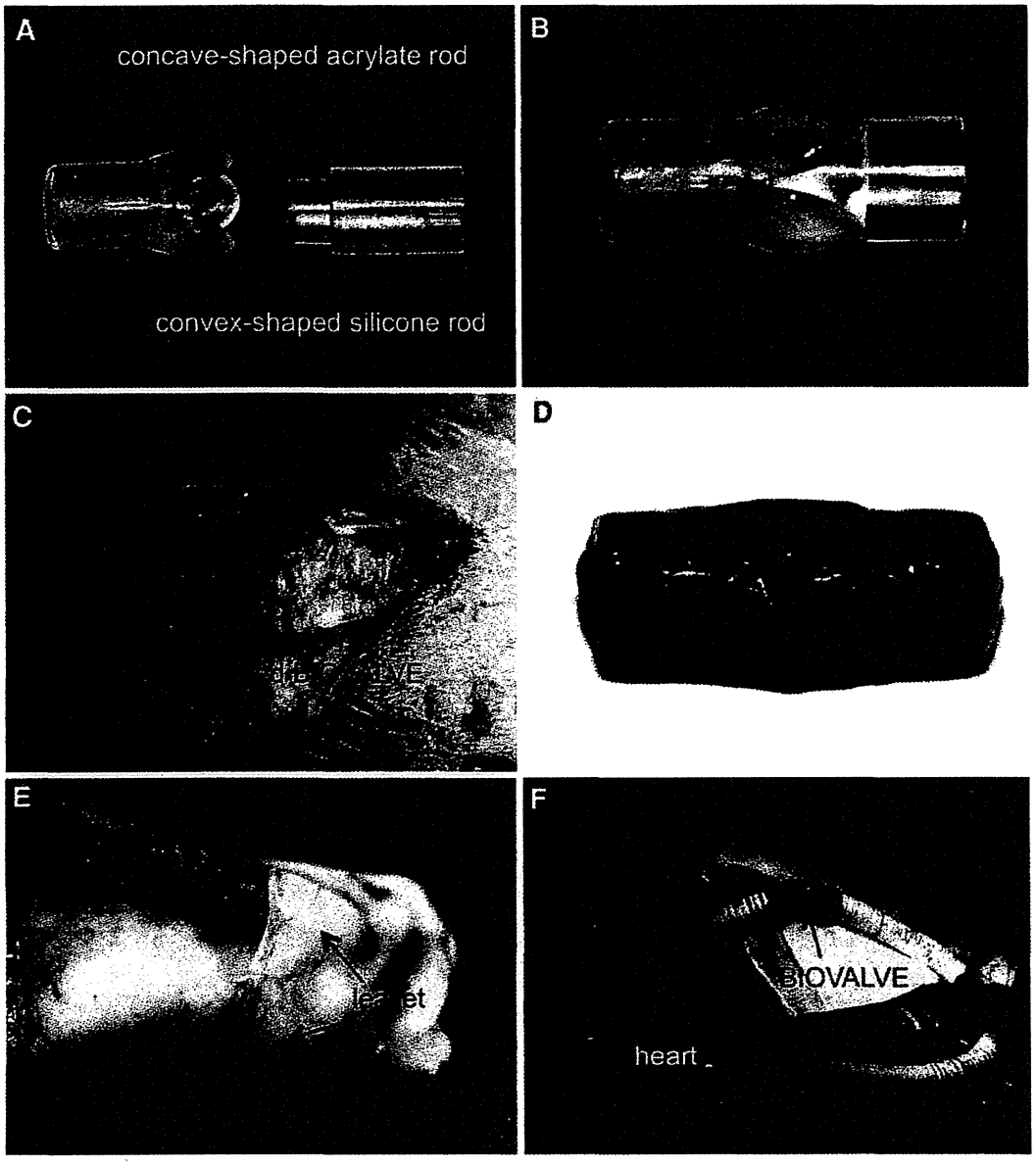

Fig. 1 Specially designed mold for the biovalve (**b**) assembled from a concave-shaped acrylate rod and a convex-shaped silicone rod (**a**) with a small 0.5-mm aperture for the formation of the leaflets. The concave-shaped rod contains three removable projections resembling the protrusions of the sinus of Valsalva. The molds were embedded for 2 months in a dorsal subcutaneous pouch in a goat. **c** After 8 weeks of implantation, the mold was encapsulated by connective tissue to form the biovalve (**d**). After removing the molds from each end of the implant, three thin leaflets were observed in the luminal side of the conduit. **e** Macroscopic observation of the formed leaflets after inversion of the biovalve conduit. **f** The biovalve was implanted between the apical portion of the left ventricle and descending aorta with interposition of ePTFE grafts without the use of cardiopulmonary bypass

In vivo evaluation of biovalves in the systemic circulation

To evaluate the biovalve under systemic circulation, we conducted an apico-aortic bypass with interposition of vascular grafts in the goat. Anesthesia was induced with 10 mg/kg of ketamine and maintained with 1–3 % isoflurane. The heart was exposed through a left thoracotomy at the fifth subcostal region. A valved conduit was composed of 14-mm ringed expanded polytetrafluoroethylene (ePTFE) grafts (GORE-TEX, W.L. Gore & Associates, Inc., Newark, DE). After treatment with a 1 % saline solution of water-soluble argatroban, a biovalve was sewed end to end to the ringed ePTFE grafts at both ends using a running 5-0 non-absorbable

suturing technique. The distal end of the valved conduit (ringed ePTFE grafts with the biovalve) was sewed end to side to the descending aorta using a partial occluding clamp and a running 4-0 non-absorbable suturing technique. An apical left ventricle connector was composed of a custom-made stainless steel conduit (outer diameters of 20 and 14 mm at either end) and a 14-mm ringed ePTFE graft. A felt cuff was sewed to the left ventricular (LV) apex with 2-0 polyester sutures with a felt strip. After injection of heparin sodium (200 U/kg), the LV apex was cored with a 19-mm custom-made ventricular coring device. Then, the apical left ventricle connector was inserted through the felt cuff into the LV apex without cardiopulmonary bypass and tied on the felt cuff. The apical left ventricle connector was sewed end to end to the valved conduit (ringed ePTFE grafts with the biovalve) using a running 4-0 non-absorbable suture technique to complete the bypass. Finally, the descending aorta was ligated with vessel tape at the proximal portion of the anastomosis of the valved conduit so that all of the blood flow to the abdominal aorta was supplied from the apico-aortic bypass.

An angiography was performed after implantation. The valve function was evaluated using transthoracic Doppler echocardiography every week. Bypass flow was continuously monitored using electromagnetic and transonic flow meters, the probes of which were attached around the ePTFE grafts.

Postoperative systemic anticoagulation for the ePTFE grafts was maintained with oral administration of warfarin sodium and aspirin.

Histological evaluation

The biovalve specimens acquired after implantation were fixed with 10 % formalin, embedded in paraffin, sliced into longitudinal sections, and finally stained with hematoxylin-eosin or Elastica van Gieson. In addition, a few sections of biovalve were also stained for α-smooth muscle actin (α-SMA) and factor VIII by immunohistochemical techniques; these proteins were detected using monoclonal antibodies (Dako Japan, Kyoto, Japan).

Statistics

Quantitative data were represented as mean ± standard deviation.

Results

Preparation and properties of biovalves

The assembled molds (Fig. 1b) embedded in the subcutaneous pouches of a goat for 2 months showed complete encapsulation with the connective tissue and marked neovascularization (Fig. 1c). The implants were easily harvested because only very fragile, irregular, and redundant tissues connected the developed biovalves and surrounding subcutaneous tissues, which could be dissected easily (Fig. 1d). The convex and concave rods were smoothly removed from each end of the implant because there was no adhesion between the molds and biovalves. The conduit had three protrusions, which were formed because of the shape of the concave substrate, resembling the sinus of Valsalva. A membranous tissue in the shape of a trileaflet was formed at the aperture of the combined rods, as intended by its design (Fig. 1e).

Analysis of the video data showed that the biovalve leaflets closed rapidly and tightly in synchronization with the backward flow in the diastolic phase (Fig. 2). In the transition phase of the flow direction, the valve opened smoothly and fully without flapping or hitting the conduit wall. The regurgitation ratio and orifice ratio were 12.0 and 82.7 %, respectively.

The strength and modulus of the leaflet part of the biovalve were 830 ± 270 and 1083 ± 289 kPa, which were almost equal to the native values, whereas in the conduit part, the strength and modulus of the biovalve were about five times larger than those of the native aorta (Fig. 3a, c). The biovalve had excellent suppleness similar to the native valve (Fig. 3b).

Application

The biovalve was implanted into an apico-aortic bypass by end-to-end anastomosis (Fig. 1f). After declamping, the implanted valve pulsated with little bleeding. An angiograph after implantation revealed good passage of blood flow and no regurgitation at the level of the biovalve (Fig. 4).

The valve function was evaluated using transthoracic Doppler echocardiography every week. Up to 2 months after implantation, echocardiographic examination revealed protrusions similar to the sinus of Valsalva and rapid opening (Fig. 5a) and closing (Fig. 5b) of the leaflets, and Doppler echocardiography (Fig. 5c) did not yield substantial evidence of stenosis and regurgitation.

The bypass flow by the electromagnetic flow meter was 2.6 ± 1.1 l/min throughout the experiment. A graph of flow waveform almost 2 months after implantation was presented in Fig. 6. The waveform has been maintained compared to pre-implanted pulsatile flow waveforms in Fig. 2.

In the 2 months after implantation, the goat was euthanized, and the biovalve implants were harvested. Macroscopic observation revealed that the shape and size of the leaflets were well maintained compared to those of native heart valve leaflets.

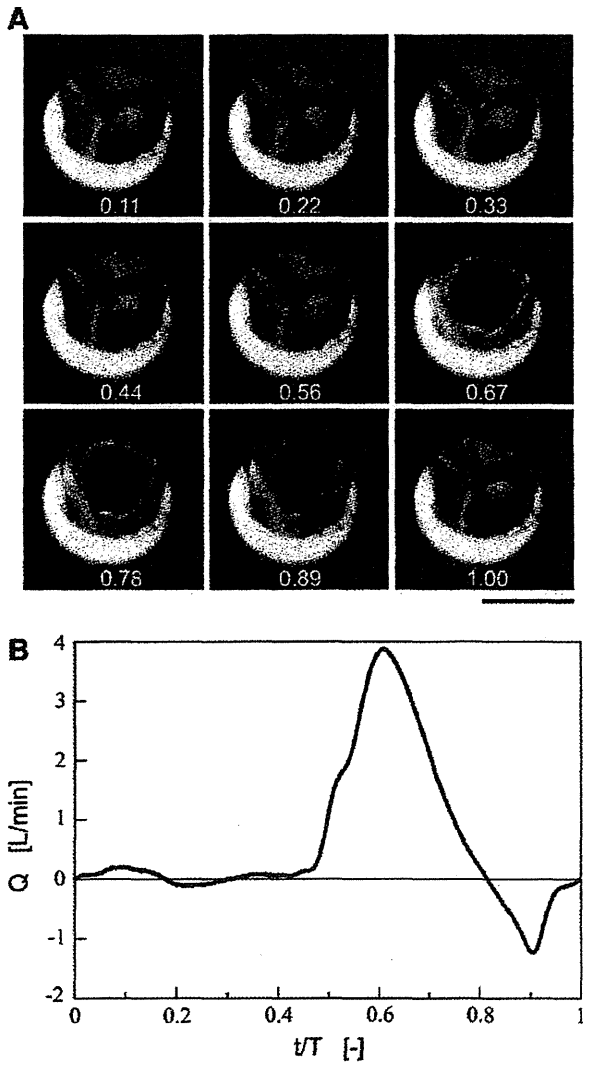

Fig. 2 **a** Valve movement under pulsatile conditions in one cycle ($T = 0.97$ s). The pulsatile rate was 62 bpm, and the average flow rate was 627 ml/min. The numbers in the photos are time/T. *Bar* 10 mm. **b** Pulsatile flow waveforms in one cycle

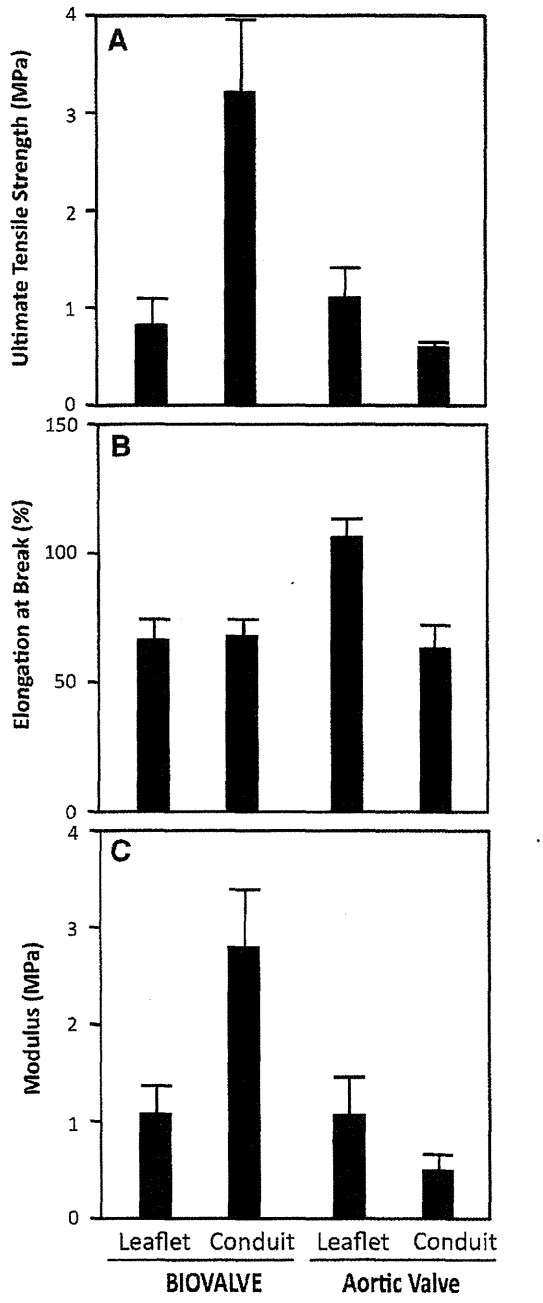

Fig. 3 Comparison of mechanical properties between biovalves and goat aortic valves. **a** The ultimate tensile strength, indicative of tissue strength, and **b** elongation at the break, indicative of tissue extensibility, were obtained from the stress-strain curves. **c** The modulus, indicative of tissue stiffness, was calculated as the slope of the linear part of the stress-strain curves. The error bars represent mean ± standard deviation ($n = 9$)

Histological evaluation

The whole body of the biovalve before implantation, including the valve leaflets and conduit, was mainly composed of collagen-rich tissue with fibroblasts (Fig. 7a). There were few elastic fiber and vascular cells. After implantation, wall thickness at the conduit and sinus of Valsalva significantly increased without any stenosis of the conduit (Fig. 5b), whereas leaflet thinness was well maintained (Fig. 7b). The conduit possessed a large amount of neovascularization (Fig. 7c). At the sinus, a thick elastic fiber formed although the main extracellular component was still collagen (Fig. 7d). Predominant cell types observed at the medial layer of the entire conduit walls included α-SMA positive, smooth muscle cells, and

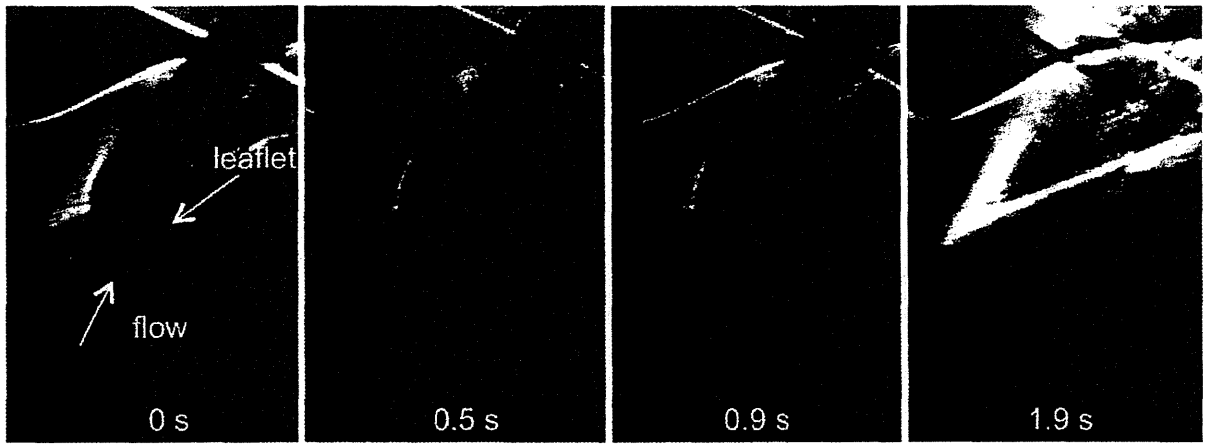

Fig. 4 Angiography performed immediately after biovalve implantation. Good passage of blood flow and no regurgitation at the level of the biovalve were observed

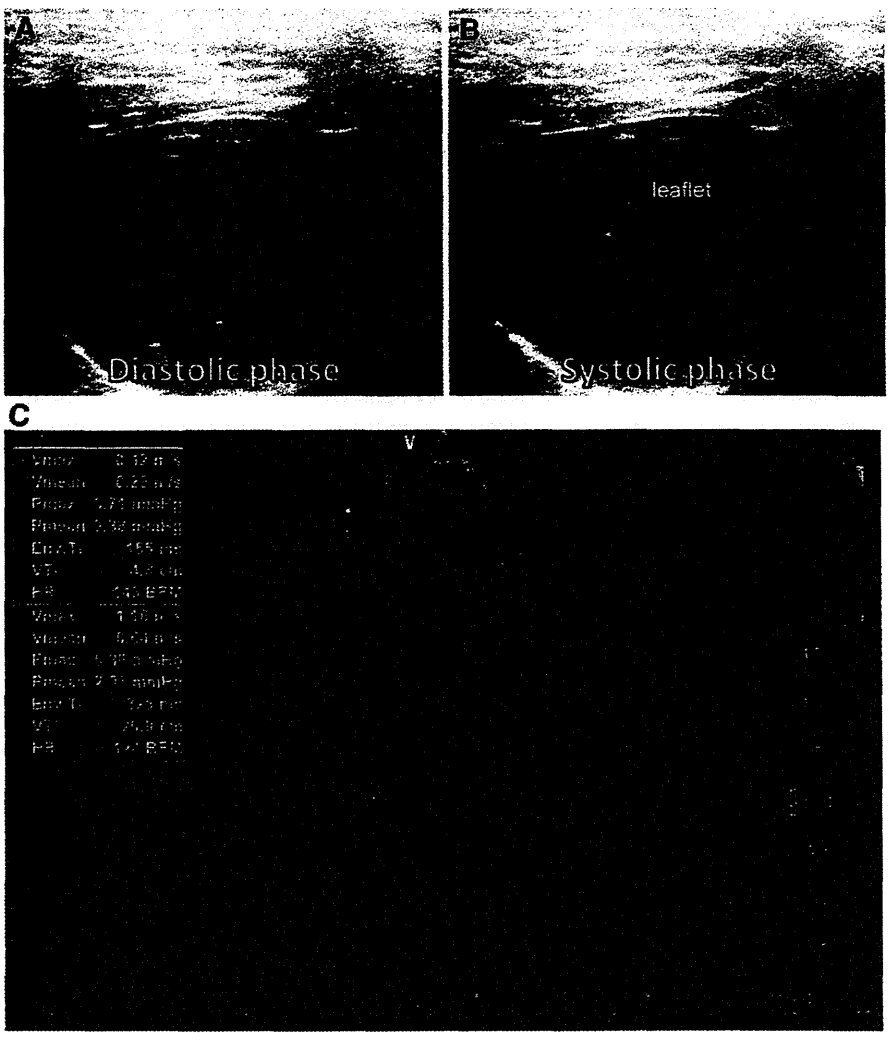

Fig. 5 Transthoracic echocardiography at 2 months after implantation of the biovalve indicated smooth leaflet movement at the opened (**a**) and closed (**b**) positions. The color Doppler echo (**c**) showed good forward flow at the systolic phase and trivial regurgitation at the diastolic phase

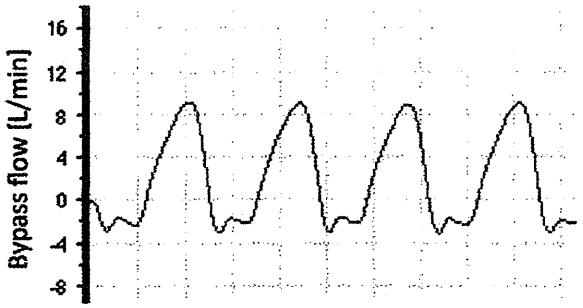

Fig. 6 A graph of flow waveform by the electromagnetic flow meter almost 2 months after implantation. The valve function has been almost maintained for 2 months

myofibroblasts (Fig. 7e–g) migrating toward the tip of the leaflet (Fig. 7h). Although the luminal surface was not covered with endothelial cells yet, no thrombus formation was observed on the smooth pseudointima (Fig. 7e, f).

Discussion

Biovalves were implanted into the systemic circulation as a pilot study with a limited experiment number and follow-up time in a goat model, although the sheep model is accepted by the FDA or other agencies as the most favorable model with regard to biodegradation/calcification. However, this is the first study reporting successful implantation of completely autologous tissue-valved conduits with no artificial support materials to the systemic circulation as aortic valves.

Due to the enormous number of patients suffering from aortic valve diseases, constructing aortic TEHVs has been the major study focus of many research groups. However, one of the predominant limitations for the development of an aortic TEHV is the use of an appropriate animal model for testing in the physiologically systemic circulation. Even in large animals, the anatomical implantation of the aortic valve conduit requires complex procedures such as cardiopulmonary bypass (CPB) and coronary arterial reconstruction. Therefore, in many previous studies, the prosthetic valves were implanted in the descending aorta [15, 16], where the pressure and flow pattern were completely different from the outflow of the left ventricle. Since implanted valves do not usually close tightly enough in this condition, valvular degeneration is often promoted. For this reason, our in vivo evaluation of biovalves in the systemic circulation with an apico-aortic bypass is worth reporting. Others have implanted the aortic valve in the pulmonary position, thus excluding the influence of systemic pressure on the implanted grafts from the beginning [17]. We have already reported successful implantation of the biovalves to the pulmonary valve position under CPB in a beagle model [13]. In a low-pressure condition, the biovalves functioned as pulmonary valves for 3 months with valvular tissue reconstruction. In this study, a potential of the biovalve as an aortic TEHV has been further increased.

The evaluation of valve function in vitro was performed under the pulsatile condition of 62 bpm with a flow rate of 627 ml/min. The condition was set for the implantation to goats weighing of about 40–50 kg, in which the average cardiac outflow is about 3.2–4.0 l/min (measured bypass flow: 2.6 ± 1.1 l/min) at a heart rate of 70–90 bpm. In the pulsatile flow circuit model, saline solution was selected as a working fluid for prevention of injury in biovalves made of natural tissues. The kinetic viscosity of blood is 4.44×10^{-6} m^2/s, which is about four times more than that of saline solution (1.00×10^{-6} m^2/s). Therefore, the flow condition in the circuit between the two different fluids, which is defined by the Reynolds number and Womersley number, needed to be adjusted for the evaluation of valve function using saline solution. The pulsatile rate and the flow rate calculated by the two numbers were 17.5–22.5 bpm and 800–1,000 ml/min (650 ± 275 l/min at the bypass), respectively.

Our biovalves were able to withstand systemic pressures without suffering structural or functional deterioration for as long as 2 months. The robust and elastic properties were obtained by slight treatment with diluted glutaraldehyde, which has been used clinically in porcine aortic valve or aortic valve repair. By designing a novel mold that reorganized biovalve construction, we developed the type VI biovalve, which demonstrates nearly perfect valve function. The key difference between the type V and VI molds is the aperture shape for leaflet formation. By preparing the valve leaflets in the open form, less regurgitation and an increase in the orifice ratio were observed upon in vitro examination. Furthermore, little regurgitation and no significant stenosis were confirmed during the observation period.

Since the biovalve was isolated from the heart and vascular tissues by ePTFE grafts in this model, α-SMA-positive cells that appeared in the conduit wall might have migrated from the surrounding connective tissue or could have originated from the fibroblasts existing in the biovalve wall since they were implanted. Further study is necessary to investigate their origin.

Regarding biovalve preparation for implantation, we followed the method of treatment with glutaraldehyde described by Duran et al. [18–22] for an aortic valve repair using an autologous pericardium leaflet. They explained that treated pericardium is used to increase the height of native aortic valve leaflets and commissures resulting in an increase in the coaptation zone. Glutaraldehyde treatment can provide more resistance against retraction and

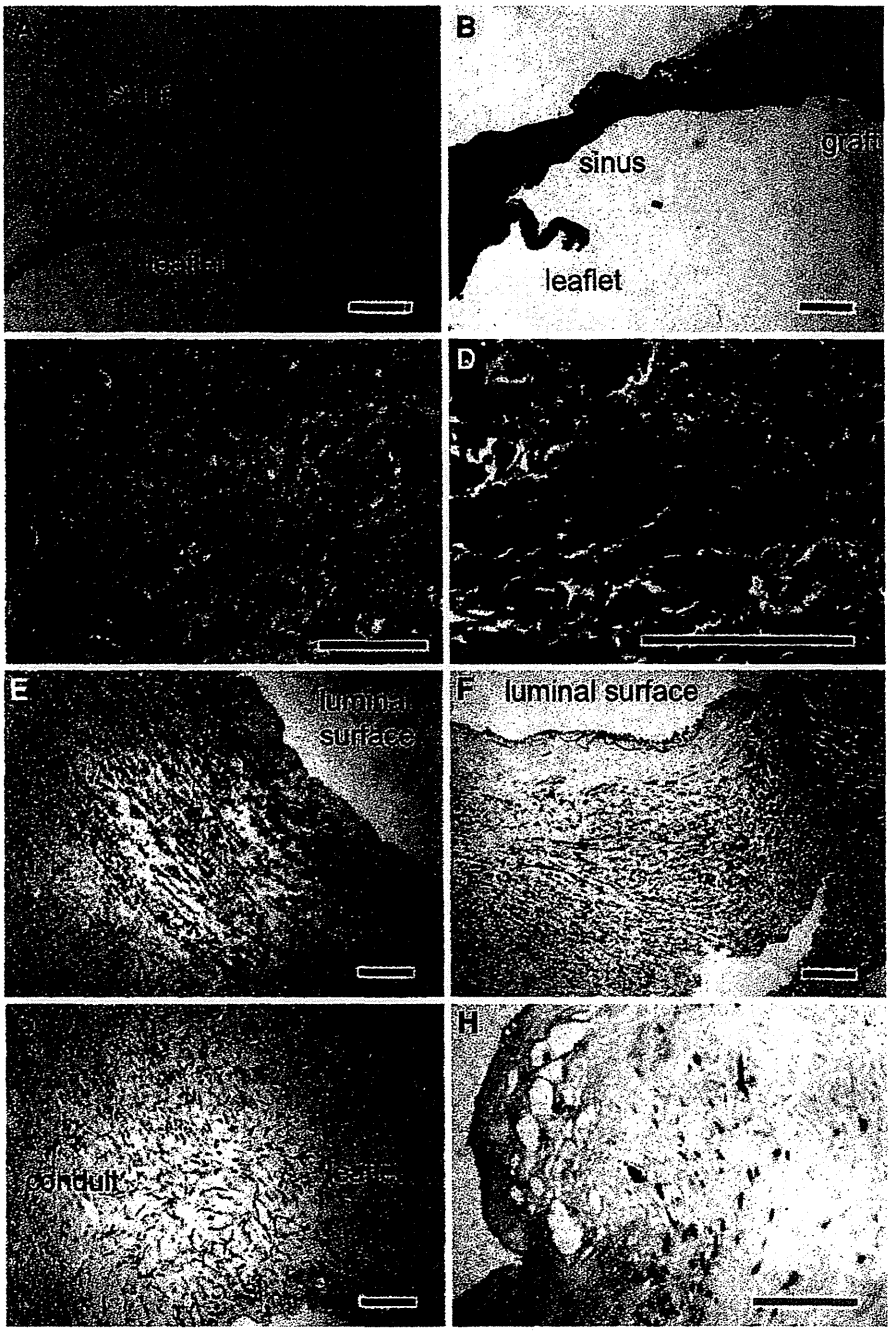

Fig. 7 Longitudinal sections of biovalve tissue before (**a**) and after (**b**) implantation (hematoxylin and eosin stain, *bar* 2 mm). **c** Neovascularization at the implanted biovalve conduit (hematoxylin and eosin stain, *bar* 100 μm). **d** Elastica van Gieson staining revealed a *black-colored* thick elastic fiber in the sinus region (*bar* 100 μm). Immunohistological staining for α-SMA revealed that predominant smooth muscle cells or myofibroblasts were observed at the sinus region (**e**), the proximal anastomosis region (**f**), and base (**g**) and tip (**h**) of the leaflet (*bar* 100 μm)

degeneration and maintain the intrinsic tissue pliability of the pericardium. However, treatment with glutaraldehyde may destroy native cells and cause denaturation of connective tissue even though the immersion is at a low dose and for a short time. Further examination is needed to determine the optimal method for biovalve preparation.

At 2 months after implantation, there were few endothelial cells at the luminal surface, whereas no thrombus formation was observed. Implantation of the biovalve at the aortic root or directly anastomosed to the native aorta was expected to result in the rapid migration of both endothelial and mesenchymal cells from the anastomotic sites, leading to quick tissue organization and maturation. This was observed in the anatomically implanted beagle model. Further implantation experiments with longer observational periods are ongoing.

Conclusion

Completely autologous type VI biovalves with robust and elastic characteristics appropriate for aortic valve replacement were developed by in-body tissue architecture technology using an improved mold design. Slight glutaraldehyde treatment enabled the type VI biovalve to achieve desirable idealistic mechanical properties for aortic valve replacement with respect to both valvular function and surgical handling. The biovalves withstood systemic pressure without unexpected dilatation or aneurysm formation in the conduit portion and degeneration or sclerosis of the valvular leaflet, which could be responsible for aortic valve regurgitation or stenosis within 2 months of implantation. Rapid tissue maturation with elastic fiber formation and the predominant appearance of α-SMA-positive cells in the completely autologous tissue without synthetic support materials might induce the growth potential of the valves.

Acknowledgments The authors thank Ms. Manami Sone, Mr. Yuji Shimakawa, and Dr. Yue-Min Zhou for their participation in this study. This study was funded in part by a Grant-in-Aid for Scientific Research (B19390368, B21360123) from the Ministry of Education, Culture, Sports, Science and Technology of Japan.

References

1. Cosgrove DM, Lytle BW, Taylor PC, Camacho MT, Stewart RW, McCarthy PM, Miller DP, Piedmonte MR, Loop FD. The Carpentier-Edwards pericardial aortic valve. Ten-year results. J Thorac Cardiovasc Surg. 1995;110:651–62.
2. Shin'oka T, Ma PX, Shum-Tim D, Breuer CK, Cusick RA, Zund G, Langer R, Vacanti JP, Mayer JE. Tissue-engineered heart valves. Autologous valve leaflet replacement study in a lamb model. Circulation. 1996;94:164–8.
3. Dohmen PM, Ozaki S, Nitsch R, Yperman J, Flameng W, Konertz W. A tissue engineered heart valve implanted in a juvenile sheep model. Med Sci Monit. 2003;9:97–104.
4. Vesely I. Heart valve tissue engineering. Circ Res. 2005;97:743–55.
5. Baraki H, Tudorache I, Braun M, Höffler K, Görler A, Lichtenberg A, Bara C, Calistru A, Brandes G, Hewicker-Trautwein M, Hilfiker A, Haverich A, Cebotari S. Orthotopic replacement of the aortic valve with decellularized allograft in a sheep model. Biomaterials. 2009;30:6240–6.
6. Nakayama Y, Ishibashi-Ueda H, Takamizawa K. In vivo tissue-engineered small-caliber arterial graft prosthesis consisting of autologous tissue (biotube). Cell Transplant. 2004;13:439–49.
7. Watanabe T, Kanda K, Ishibashi-Ueda H, Yaku H, Nakayama Y. Development of biotube vascular grafts incorporating cuffs for easy implantation. J Artif Organs. 2007;10:10–5.
8. Sakai O, Kanda K, Ishibashi-Ueda H, Takamizawa K, Ametani A, Yaku H, Nakayama Y. Development of the wing-attached rod for acceleration of "Biotube" vascular grafts fabrication. J Biomed Mater Res B Appl Biomater. 2007;83:240–7.
9. Watanabe T, Kanda K, Ishibashi-Ueda H, Yaku H, Nakayama Y. Autologous small-caliber "Biotube" vascular grafts with argatroban loading: a histomorphological examination after implantation to rabbits. J Biomed Mater Res B Appl Biomater. 2010;92:236–42.
10. Hayashida K, Kanda K, Yaku H, Ando J, Nakayama Y. Development of an in vivo tissue-engineered, autologous heart valve (the biovalve): preparation of a prototype model. J Thorac Cardiovasc Surg. 2007;134:152–9.
11. Hayashida K, Kanda K, Oie T, Okamoto Y, Ishibashi-Ueda H, Onoyama M, Tajikawa T, Ohba K, Yaku H, Nakayama Y. Architecture of an in vivo-tissue engineered autologous conduit "Biovalve". J Biomed Mater Res B Appl Biomater. 2008;86:1–8.
12. Nakayama Y, Yamanami M, Yahata Y, Tajikawa T, Ohba K, Watanabe T, Kanda K, Yaku H. Preparation of a completely autologous trileaflet valve-shaped construct by in-body tissue architecture technology. J Biomed Mater Res B Appl Biomater. 2009;91:813–8.
13. Yamanami M, Yahata Y, Uechi M, Fujiwara M, Ishibashi-Ueda H, Kanda K, Watanabe T, Tajikawa T, Ohba K, Yaku H, Nakayama Y. Development of a completely autologous valved conduit with the sinus of valsalva using in-body tissue architecture technology: a pilot study in pulmonary valve replacement in a beagle model. Circulation. 2010;122:S100–6.
14. Nakayama Y, Yahata Y, Yamanami M, Tajikawa T, Ohba K, Kanda K, Yaku H. A completely autologous valved conduit prepared in the open form of trileaflet (type VI biovalve): mold design and valve function in vitro. J Biomed Mater Res Part B Appl Biomater. 2011;99B:135–41.
15. Conconi MT, Rocco F, Spinazzi R, Tommasini M, Valfrè C, Busetto R, Polesel E, Albertin G, Dei Tos A, Iacopetti I, Cecchetto A, Zussa C, Grigioni M, Parnigotto PP, Nussdorfer GG. Biological fate of tissue-engineered porcine valvular conduits xenotransplanted in the sheep thoracic aorta. Int J Mol Med. 2004;14:1043–8.
16. Gulbins H, Pritisanac A, Pieper K, Goldemund A, Meiser BM, Reichart B, Daebritz S. Successful endothelialization of porcine glutaraldehyde-fixed aortic valves in a heterotopic sheep model. Ann Thorac Surg. 2006;81:1472–9.
17. Van Nooten G, Somers P, Cornelissen M, Bouchez S, Gasthuys F, Cox E, Sparks L, Narine K. Acellilar porcine and kangaroo aortic valve scaffolds show more intense immune-mediated calcification than cross-linked Toronto SPV valves in the sheep model. Interact Cardiovasc Thorac Surg. 2006;5:544–9.
18. Duran CMG, Alonso J, Gaite L, Alonso C, Cagigas JC, Marce L, Fleitas MG, Revuelta JM. Long-term results of conservative repair of rheumatic aortic valve insufficiency. Eur J Cardiothorac Surg. 1988;2:217–23.
19. Duran CM, Gometza B, Kuma N, Gallo R, Bjonastad K. From aortic cusp extension to valve replacement with stentless pericardium. Ann Thorac Surg. 1995;60:S428–32.
20. Duran CMG, Gometza B, Kuma N. Aortic valve replacement with freehand autologous pericardium. J Thorac Cardiovasc Surg. 1995;110:511–6.
21. Duran C, Gometza B, Kuma N, Gallo R, Bjonastad K. Treated bovine and autologous pericardium: surgical technique. J Cardiac Surg. 1995;10:1–9.
22. Ozaki S, Kawase I, Yamashita H, Uchida S, Nozawa Y, Matsuyama T, Takatoh M, Hagiwara S. Aortic valve reconstruction using self-developed aortic valve plasty system in aortic valve disease. Interact Cardiovasc Thorac Surg. 2011;12:550–3.

2/3 冊

厚生労働科学研究費補助金

難病・がん等の疾患分野の医療の実用化研究事業

Bridge to Decision を目的とした超小型補助循環システム並びに頭蓋内・心血管治療用の新規多孔化薄膜カバードステントに関する医師主導型治験及び実用化研究

平成 24 年度総括・分担研究報告書

研究代表者　　峰松　一夫

平成 25　(2013)年　　5 月

J Artif Organs (2012) 15:11–19
DOI 10.1007/s10047-012-0633-9

REVIEW

Journal of Artificial Organs 2011: the year in review

Journal of Artificial Organs Editorial Committee

Received: 1 February 2012 / Published online: 29 February 2012

Introduction

We are pleased to introduce to colleagues worldwide, through the publication *Journal of Artificial Organs* (JAO), a wide range of important new achievements in the field of artificial organs, ranging from fundamental research to clinical applications. We believe the JAO has very high potential for promoting interest and research in artificial organs not only in Japan but also in other parts of the world, and the specialization, originality, and level of science in the journal are at the highest levels in the field.

An electronic version of the JAO has been available through our publisher's electronic publishing system since 2002. The full-text journal is accessible at more than 4,000

Y. Sawa
Division of Cardiovascular Surgery, Department of Surgery, Osaka University Graduate School of Medicine, 2-2 Yamadaoka, Suita, Osaka 565-0871, Japan
e-mail: sawa@surg1.med.osaka-u.ac.jp

E. Tatsumi · T. Tsukiya
Department of Artificial Organs, National Cerebral and Cardiovascular Center Research Institute, Suita, Osaka, Japan

A. Funakubo
Department of Electronic and Computer Engineering, School of Science and Engineering, Tokyo Denki University, Tokyo, Japan

T. Horiuchi
Department of Chemistry for Materials, Faculty of Engineering, Mie University, Tsu, Japan

K. Iwasaki
Waseda Institute for Advanced Study, Waseda University, Tokyo, Japan

A. Kishida
Institute of Biomaterials and Bioengineering, Tokyo Medical and Dental University, Tokyo, Japan

T. Masuzawa
Department of Mechanical Engineering, Ibaraki University, Hitachi, Japan

K. Matsuda
Emergency and Critical Care Medicine, University of Yamanashi Hospital, Chuo, Japan

A. Myoui
Medical Center for Translational Research, Osaka University Hospital, Osaka, Japan

M. Nishimura
Division of Organ Regeneration Surgery, Tottori University Faculty of Medicine, Yonago, Japan

T. Nishimura
Department of Therapeutic Strategy for Heart Failure, The University of Tokyo, Tokyo, Japan

S. Tokunaga
The Department of Cardiovascular Surgery, Kanagawa Cardiovascular and Respiratory Center, Yokohama, Japan

Y. Tomizawa
Department of Cardiovascular Surgery, Tokyo Women's Medical University, Tokyo, Japan

T. Tomo
Second Department of Internal Medicine, Faculty of Medicine, Oita University, Yufu, Japan

T. Yamaoka
Department of Biomedical Engineering, National Cerebral and Cardiovascular Center Research Institute, Suita, Japan

Journal of Artificial Organs Editorial Committee (✉)
Osaka, Japan
e-mail: sawa@surg1.med.osaka-u.ac.jp

institutes and libraries throughout the world. Furthermore, an "Online First" service has been introduced to JAO from Volume 13, Number 1 issue. Online First publishes accepted articles in electronic form before the appearance of the printed journal, without having to wait for the completion of an entire issue. This means a significant reduction in publication time, which is approximately 35 days according to the recent statistical data.

From the beginning with Volume 1 in 1998 to the last issue in 2010, papers from 19 different countries were accepted for publication in JAO. In 2008, JAO was accepted for abstracting and indexing in the Web of Science/Citation Index Expanded by Thompson Reuters, and in 2010, JAO obtained the first impact factor of 1.532. The second year impact factor announced in the Journal Citation Reports for 2010 remained almost unchanged at 1.488. We were very proud of this impact factor, which was the culmination of a long-term process of more than a decade. Since we obtained the impact factor, the number of papers submitted to our journal has increased substantially.

In 2006, we started to review and summarize all the articles published in the past year in the JAO, to facilitate an overview for our readers [1–6]. This practice has continued this year also, and the articles published in Volume 14, 2011 are summarized below. In this volume, we published 57 articles including 35 original papers, 2 review papers, 1 mini review, 11 case reports, 6 brief communications, and 1 letter to the editor. These papers were related to many aspects of basic research on, and development and clinical applications of artificial organs, and covered a variety of subfields including artificial hearts, cardiopulmonary bypass, blood vessel prosthesis, artificial valves, dialysis, apheresis, artificial pancreas, retinal prosthesis, biomaterials, tissue engineering, regeneration therapy, etc. A total of 140 reviewers who are specialists in artificial organs helped our authors to improve their manuscripts by means of thoughtful reviews, critiques, and suggestions. We are pleased to present such excellent work in our journal.

We thank all authors, reviewers, and members, and hope they will continue to support our journal.

Artificial heart (basic)

Mitamura et al. of Tokai University developed a magnetic fluid seal which has a shield mechanism for rotary blood pumps and evaluated the sealing performance of the magnetic fluid seal. The magnetic fluid seal with a shield had long-term durability of 275 days [7].

Tanaka et al. of the National Cardiovascular Center reported an implantable, compact rotary blood pump using an axial turbo pump with hydrodynamic bearings. The pump was installed in four calves for up to 90 days to evaluate hemodynamic performance and biocompatibility. The pump stably produced a flow of 5 l/min, with no incidence of hemorrhage, organ failure, or significant hemolysis. No thrombus formation or mechanical wearing was observed inside the pump [8].

Ando et al. reported their novel method for estimating cardiac function with continuous flow LVAD, for possible explantation of the device after myocardial recovery. They carried out a series of animal experiments to establish a unique varied-speed driving mode in synchronization with ECG signals [9].

Ando et al. of the National Cardiovascular Center reported the effect of a novel control method for left ventricular assist devices (LVAD) on intracircuit backward flow during pump weaning. They have developed a drive mode of centrifugal pumps that can change its rotational speed in synchronization with cardiac cycle of the native heart. They drove a centrifugal pump in a mock circulation and evaluated the effect of the counterpulse mode, which increases pump speed in diastole only. The counterpulse mode significantly reduced the amount of pump backward flow compared with the continuous mode. They concluded that the novel drive mode can reduce LVAD backward flow during pump weaning and can be beneficial for safe and proper pump-off trials [10].

Shi et al. of the University of Tokyo proposed an automatic algorithm for calibration of the inlet pressure sensor from the pressure waveform in the condition of ventricle sucking for the implantable continuous-flow ventricular-assist device. The calibration algorithm was constructed on the basis of two considerations. First, intrathoracic pressure could be substituted for atmospheric pressure because the lung is open to air. Second, the inlet pressure at the release point of sucking would represent the intrathoracic pressure, because the atrial pressure would be low owing to the sucking condition. A special mock circulation system that can reproduce ventricle sucking was developed to validate the calibration algorithm. The calibration algorithm worked well with a maximum SD of 2.1 mmHg for 3-min measurement in the mock circulation system [11].

Kosaka et al. of the National Institute of Advanced Industrial Science and Technology invented a new method for measurement of flow rate for an implantable axial blood pump. A miniaturized mass-flow meter, which makes use of centrifugal force produced by the mass-flow rate around a curved cannula made of titanium alloy, was developed and evaluated in in-vitro tests, and compared with a conventional flow meter. Measurement error was less than ±0.5 l/min and average time delay was 0.14 s [12].

Ando et al. of the National Cerebral and Cardiovascular Center Research Institute revealed that a counterpulsation mode of rotary left ventricular assist devices can enhance

myocardial perfusion. A novel pump controller that can change its rotational speed (RS) in synchronization with the native cardiac cycle and the Evaheart LVAD was installed by the left ventricular uptake and the descending aortic return. Coronary flow was compared under four conditions: circuit-clamp, continuous mode (constant pump speed), counterpulse mode (increased pump speed in diastole), and copulse mode (increased pump speed in systole). In counterpulse mode, coronary flow increased significantly compared with that in continuous mode. The counterpulse drive mode, which increases pump speed in diastole mode, can provide great benefits to patients with end-stage heart failure, especially those with ischemic etiology [13].

Yamada et al. reported a newly developed neointima-inducing inflow cannula designed to enhance autologous neointima formation over the inflow cannula inside the ventricle and, consequently, to prevent the wedge thrombus around the penetration site. They use a novel titanium mesh to wrap the cannula tip. They evaluated the cannula in a series of animal studies, and the histological findings showed that the neointimal tissue consisted of a layer of endothelial cells and fibroblasts after 2 months [14].

Mizuno et al. reported the development of a novel skin-button system to prevent driveline infection of implantable LVADs. The newly developed skin-button consists of two flanges made of tissue-compatible segmented polyurethane. The combination of these two flanges with different features enables the driveline to fix on the skin without epithelial downgrowth and peridriveline pocket formation, and can prevent bacterial infection over a prolonged period. They proved the effectiveness of the device in chronic animal experiments with an implantable LVAD for 90 days [15].

Tsukiya et al. reported an analysis of the flow field of a newly developed inflow cannula that was designed for a bridge-to-decision system. The cannula's unique configuration composed of elasticized struts and side slits contributed to the small hydraulic resistance of the cannula. The computed flow field revealed the existence of the low shear rate region on the inner surface of the cannula, which should be considered in the discussion of anticoagulant therapy for patients with LVAD using this cannula [16].

Artificial heart (clinical)

DuraHeart is the first clinically available magnetically levitated implantable centrifugal pump in the world. Kurihara et al. reported the first successful bridge-to-transplant case using DuraHeart in Japan after 437 days of support. Mediastinitis is a devastating complication after open heart surgery [17].

Kurihara et al. described a case in which sternal infection after VAD implantation was successfully treated by rerouting the outflow vascular graft to the descending aorta. The emerging field of regenerative medicine, which uses human cells and tissues to regenerate internal organs, is now advancing from basic and clinical research to clinical application [18].

Kawata et al. of The University of Tokyo reported two cases of successful use of negative pressure wound therapy (NPWT) to control LVAD-related mediastinitis. They experienced two cases of mediastinitis after LVAD implantation, and successfully treated them with NPWT using hydrophilic polyurethane foam. They concluded that NPWT might become a preferred therapeutic option for control of LVAD-related mediastinitis [19].

Anthracyclines are effective antineoplastic drugs, but are known to be cardiotoxic. Recovery of cardiac function is rare. Kurihara et al. reported a bridge to recovery of ventricular function, using VAD implantation for anthracycline-induced cardiomyopathy [20].

Inoue et al. reported use of an LVAD support with a extracorporeal centrifugal pump for 2 months in a child weighing 5 kilograms for the first time. This case report stressed the possibility of wider clinical application of rotary blood pumps for pediatric patients in need of assisted circulation [21].

Gon et al. of Tsukuba Memorial Hospital reported a case with an extracorporeal VAD who participated in a sleepover program. This patient was 19-year-old woman with fulminant myocarditis and she was treated by Toyobo VAD. After stabilizing her general condition, they conducted a sleepover program so she could attend her coming-of-age ceremony in her home town, which is 120 km from the hospital. This program was carried out by a variety of their support organizations without any adverse event [22].

Sunagawa et al. of Sakurabashi Watanabe Hospital reported a patient who survived near-fatal device-related complications after Toyobo VAD implantation. A VAD for refractory heart failure because of dilated cardiomyopathy was implanted in the patient. His postoperative course was notable for infection at the exit site of the cannula, resulting in bacteremia. At 122 days postsurgery he experienced massive cerebral hemorrhage. Because discontinuation of anticoagulation is associated with a high risk of serious thromboembolism complications, removal of the LVAD was conducted electively. Although his heart function was not fully recovered (LIVED 26%, LVEDD 48 mm), he maintained NYHA functional class II status as an outpatient over the 8-month follow-up period [23].

Kurihara et al. of The University of Tokyo reported a case in which long-term biventricular assist device (Bi-VAD) support enabled successful heart transplantation.

The patient with refractory heart failure due to dilated cardiomyopathy underwent implantation of a Toyobo Bi-VAD. She was brought to the United States on POD 189 under BiVAD support, and underwent successful heart transplantation on POD 199 [24].

Cardiopulmonary bypass

Lee et al. of Chonnam National University Hospital reported a rare case of iatrogenic ilio-iliac arteriovenous fistula after percutaneous cardiopulmonary support (PCPS). They treated an 85-year-old woman with persistent hypotension by use of PCPS, and she was separated from PCPS after circulatory stabilization. They found ilio-iliac fistula by computed tomography angiography. An endovascular covered stent was deployed at the site of the fistula, achieving successful sealing of the fistulous tract [25].

Kunihara et al. investigated cytokine balance in a hepatosplanchnic system during thoracoabdominal aortic aneurysm repair. The authors found TNF-alpha, L-FABP, and I-FABP could be produced in the hepatosplanchnic system during TAAA repair. These cytokines and fatty acid binding proteins might be useful in judging whether or not the visceral perfusion method during TAAA repair is appropriate [26].

Nakamura et al. from Jikei University Kashiwa evaluated time-related hemolysis in mediastinal shed blood stored at different temperatures (20 vs. 4°C) in clinics, for the purpose of reducing the need for homologous blood transfusion. Storage at 4°C was preferable, with regard to free Hb, to storage at 20°C [27].

Blood vessel prosthesis

Yagi et al. reported short-term function of double-raschel knitted silk vascular grafts 1.5 mm in diameter and 10 mm in length in rat abdominal aorta. The grafts were coated with silk fibroin aqueous solution containing poly(ethylene glycol diglycidyl ether) as cross-linking agent and implanted for 8 weeks [28].

Moriwaki et al. of Hokkaido University reported microscopic elastic modulus distribution in canine aorta using a scanning haptic microscope. Under no-load condition, they showed that the elastic modulus of the wall in the arterial longitudinal direction was highest on the side of the luminal surface and decreased gradually toward the adventitial side. These data were consistent with the tendency of elastic fiber density distribution observed by histological staining section of the aorta. They also revealed microscopically the elastic modulus of the aorta [29].

Artificial valve

Washiyama et al. of Hamamatsu University School of Medicine investigated the effect of hemodialysis on the outcome of heart-valve replacement, and elucidated the difference between early and midterm results of heart valve replacement according to the etiology of renal diseases. They demonstrated that midterm survival of patients with primary renal diseases (glomerulonephritis and others) seemed better than for those with secondary renal diseases (nephrosclerosis and diabetic nephropathy), despite elevated perioperative risk as a consequence of longer duration of dialysis. These results may help the choice of heart valve prosthesis for chronic dialysis patients [30].

Romata et al. of the University of Padua, Italy, designed a novel diagnostic and prognostic tool able to detect valvular thrombosis in mechanical heart valves at early stages of formation, i.e., before the appearance of critical symptoms, in patients who can be effectively treated by pharmacological therapy, preventing re-operation. The ability to detect and classify thrombotic formations on mechanical valve leaflets would enable ranking of patients by assigning them to risk classes, helping clinicians to establish adequate therapeutic approaches [31].

Kuwabara et al. of Nagoya University reviewed their clinical experience of surgery for paravalvular leakage (PVL). Between 1992 and 2009 they had 8 cases of aortic PVL and 10 subjects with mitral PVL. They demonstrated that aortic PVL occurred more frequently because of laxation of sutured threads without frequent sites. Conversely, mitral PVL was mainly caused by cutting annulus tissue around the anterior commisurae after primary MVR, and by a valve-on-valve structure on the middle scallop of the posterior leaflet or circumferentially after re-MVR. They concluded that valve-on-valve replacement, which was a major cause of PVL after re-MVR, should be avoided in a re-MVR procedure, and that cautious follow-up is necessary, even in the late phase after surgery, especially for patients who have undergone MVR [32].

Arinaga et al. of Kurume University evaluated the long-term results of their 244 patients with the Carpentier–Edwards pericardial (CEP) valve in the aortic position between January 1996 and December 2007. Actuarial survival at 5, 10, and 12 years was 85.3 ± 2.8, 80.0 ± 3.7, and 70.0 ± 9.8%, respectively. Actuarial freedom from thromboembolism, endocarditis, and reoperation at 10 years was 96.9 ± 0.14, 97.7 ± 0.16, and 97.0 ± 0.16%, respectively. They concluded that long-term results of implantation of the CEP bioprosthesis in the aortic position